

# Scalar Emission in the Bulk in a Rotating Black Hole Background

S. Creek<sup>1</sup>, O. Efthimiou<sup>2</sup>, P. Kanti<sup>1,2</sup> and K. Tamvakis<sup>2</sup>

<sup>1</sup> *Department of Mathematical Sciences, University of Durham, Science Site, South Road, Durham DH1 3LE, United Kingdom*

<sup>2</sup> *Division of Theoretical Physics, Department of Physics, University of Ioannina, Ioannina GR-45110, Greece*

## Abstract

We study the emission of scalars into the bulk from a higher-dimensional rotating black hole. We obtain an analytic solution to the field equation by employing matching techniques on expressions valid in the near-horizon and far-field regimes. Both analytic and numerical results for the absorption probability, in the low-energy and low-angular momentum limit, are derived and found to be in excellent agreement. We also compute the energy emission rate, and show that the brane-to-bulk ratio of the energy emission rates for scalar fields remains always larger than unity in the aforementioned regime.

# 1 Introduction

Theories of extra spatial dimensions [1, 2] offer hope for the resolution of the hierarchy problem arising between the scale of gravity and that of other fundamental interactions. Within this framework gravity, and possibly scalar fields, propagate in the full  $(4 + n)$ -dimensional continuum (bulk), while ordinary matter is trapped on a four-dimensional hypersurface (brane). The resolution of the hierarchy problem arises because the fundamental scale of higher-dimensional gravity can be close to the other particle physics scales, while the traditional scale of gravity (Planck mass) is related to it in terms of the volume and number of extra dimensions. In this context, *trans-planckian* collisions can give rise to potentially observable black hole creation [3]. These higher dimensional black holes [4] could be produced either in ground-based colliders or in cosmic ray interactions and detected through the emitted Hawking radiation [5]. There is a considerable amount of recent literature on the subject (see [6]) including both numerical and analytic studies of the Hawking radiation in the Schwarzschild phase [7, 8, 9, 10, 11, 12, 13, 14, 15, 16] as well as the spin-down phase [17, 18, 19, 20, 21, 22, 23, 24, 25, 26, 27, 28].

In previous articles we provided analytic results for the evaporation of higher-dimensional black holes through the emission of scalars [27], fermions and gauge bosons [28] on the brane. Here, we continue our program of analytic study by focusing on the emission of scalar degrees of freedom in the bulk from rotating higher-dimensional black holes. In section 2 we set up the general theoretical framework, considering the gravitational background corresponding to a rotating higher-dimensional black hole and writing down all relevant equations for a scalar field in such a spacetime. In section 3 we provide an analytic solution of the radial equation using a well-known matching technique. This technique consists of, first, deriving the solution in the *near horizon regime*, then deriving the equivalent *far field* limit, before finally stretching and matching the two forms in an intermediate zone. In this way an analytic expression for the radial part of the field valid throughout the entire spacetime is constructed. The solution obtained in this way is valid in the low-energy and low-angular-momentum approximation. Our solution is used in section 4 to calculate the absorption probability which characterises the emitted Hawking radiation. We also perform a complimentary numerical analysis, valid in the same regime, and compare the two sets of results. Plots are depicted for various dimensional spacetimes and angular momentum modes. In section 5 we compute the energy emission rate and the brane-to-bulk ratio of the energy emission rates, and provide corresponding plots. Finally, in section 6 we present our conclusions.

## 2 General Framework

The gravitational background around a  $(4+n)$ -dimensional, neutral, rotating black hole is described by the well-known Myers-Perry solution [4]. Here we will be interested in black holes created by an on-brane collision of particles, and may therefore assume that the corresponding metric will depend only on one non-zero angular momentum component,

parallel to our brane. Then, the line-element takes the form

$$ds^2 = -\left(1 - \frac{\mu}{\Sigma r^{n-1}}\right) dt^2 - \frac{2a\mu \sin^2 \theta}{\Sigma r^{n-1}} dt d\varphi + \frac{\Sigma}{\Delta} dr^2 + \Sigma d\theta^2 + \left(r^2 + a^2 + \frac{a^2 \mu \sin^2 \theta}{\Sigma r^{n-1}}\right) \sin^2 \theta d\varphi^2 + r^2 \cos^2 \theta d\Omega_n^2, \quad (1)$$

where

$$\Delta = r^2 + a^2 - \frac{\mu}{r^{n-1}}, \quad \Sigma = r^2 + a^2 \cos^2 \theta, \quad (2)$$

and  $d\Omega_n^2(\theta_1, \theta_2, \dots, \theta_{n-1}, \phi)$  is the line-element on a unit  $n$ -sphere. The black hole's mass  $M_{BH}$  and angular momentum  $J$  are related to the parameters  $a$  and  $\mu$  as follows

$$M_{BH} = \frac{(n+2)A_{n+2}}{16\pi G} \mu, \quad J = \frac{2}{n+2} M_{BH} a, \quad (3)$$

with  $G$  being the  $(4+n)$ -dimensional Newton's constant, and  $A_{n+2}$  the area of a  $(n+2)$ -dimensional unit sphere given by  $A_{n+2} = 2\pi^{(n+3)/2} / \Gamma[(n+3)/2]$ . Finally, the black hole's horizon radius  $r_h$  follows from the equation  $\Delta(r_h) = 0$ , and is found to satisfy the equation:  $r_h^{n+1} = \mu / (1 + a_*^2)$ , where  $a_* = a/r_h$ .

In this work we will study the emission of Hawking radiation, in the form of scalar fields, in the higher-dimensional space. We therefore need to consider the equation of motion of a massless scalar field propagating in the gravitational background (1). This is given by

$$\frac{1}{\sqrt{-g}} \partial_\mu (\sqrt{-g} g^{\mu\nu} \partial_\nu \Phi) = 0, \quad (4)$$

where

$$\sqrt{-g} = \Sigma \sin \theta r^n \cos^n \theta \prod_{i=1}^{n-1} \sin^i \theta_i. \quad (5)$$

The above equation can be separated by assuming the factorised ansatz

$$\Phi = e^{-i\omega t} e^{im\varphi} R(r) S(\theta) Y_{jn}(\theta_1, \dots, \theta_{n-1}, \phi), \quad (6)$$

where  $Y_{jn}(\theta_1, \dots, \theta_{n-1}, \phi)$  are the hyperspherical harmonics on the  $n$ -sphere that satisfy the equation [29]

$$\sum_{k=1}^{n-1} \frac{1}{\prod_{i=1}^{n-1} \sin^i \theta_i} \partial_{\theta_k} \left[ \left( \prod_{i=1}^{n-1} \sin^i \theta_i \right) \frac{\partial_{\theta_k} Y_{jn}}{\prod_{i>k}^{n-1} \sin^2 \theta_i} \right] + \frac{\partial_{\phi\phi} Y_{jn}}{\prod_{i=1}^{n-1} \sin^2 \theta_i} + j(j+n-1) Y_{jn} = 0. \quad (7)$$

The functions  $R(r)$  and  $S(\theta)$  are then found as the solutions to the decoupled equations

$$\frac{1}{r^n} \partial_r (r^n \Delta \partial_r R) + \left( \frac{K^2}{\Delta} - \frac{j(j+n-1)a^2}{r^2} - \Lambda_{j\ell m} \right) R = 0, \quad (8)$$

$$\frac{1}{\sin \theta \cos^n \theta} \partial_\theta (\sin \theta \cos^n \theta \partial_\theta S) + \left( \omega^2 a^2 \cos^2 \theta - \frac{m^2}{\sin^2 \theta} - \frac{j(j+n-1)}{\cos^2 \theta} + E_{j\ell m} \right) S = 0, \quad (9)$$

respectively, that first appeared in the literature in Ref. [30]. In the above,

$$K = (r^2 + a^2)\omega - am, \quad \Lambda_{j\ell m} = E_{j\ell m} + a^2\omega^2 - 2am\omega. \quad (10)$$

The angular eigenvalue  $E_{j\ell m}(a\omega)$  provides a link between the angular and radial equation and, as in the case of on-brane emission [27, 18, 20, 21, 24], there is no closed analytic form for its value. It may however be expressed as a power series in  $a\omega$  [31, 32]. For the purpose of our analysis, valid only in the low- $\omega$  and low- $a$  limit, it suffices to keep a finite number of terms and we will therefore truncate the series at the 5th order<sup>1</sup>. In order for the power series to converge in the limit  $a\omega \rightarrow 0$  by terminating at finite order, a number of restrictions are imposed on the allowed values of the integer parameters  $(j, \ell, m)$  specifying the emission mode: in general,  $m$  may take any integer value and  $j$  and  $\ell$  any positive or zero integer value providing [31]

$$\ell \geq j + |m| \quad \text{and} \quad \frac{\ell - (j + |m|)}{2} \in \{0, \mathbb{Z}^+\}. \quad (11)$$

By using the power series form of the angular eigenvalues, we may now proceed to solve Eq. (8) analytically. The solution for the radial function  $R(r)$  will help us determine the absorption probability  $|\mathcal{A}_{j\ell m}|^2$  for the propagation of a massless scalar field in the bulk, a quantity that characterises the Hawking radiation emission rates of the black hole.

### 3 Analytic Solution

In order to obtain a solution to the radial equation (8), we will use a well-known approximate method: we will first solve the equation close to the horizon of the black hole ( $r \simeq r_h$ ), and then far away from it ( $r \gg r_h$ ). Finally, we will smoothly match the two solutions in the intermediate zone, thus creating an analytical solution for the whole radial regime.

Starting from the near-horizon regime, we perform the following transformation of the radial variable [27, 28]

$$r \rightarrow f(r) = \frac{\Delta(r)}{r^2 + a^2} \Rightarrow \frac{df}{dr} = (1 - f) r \frac{A(r)}{r^2 + a^2}, \quad (12)$$

where  $A(r) \equiv (n + 1) + (n - 1) a^2/r^2$ . Then, near the horizon ( $r \simeq r_h$ ), Eq. (8) takes the form

$$f(1-f) \frac{d^2 R}{df^2} + (1 - D_* f) \frac{dR}{df} + \left[ \frac{K_*^2}{A_*^2 f(1-f)} - \frac{(j(j+n-1)a_*^2 + \Lambda_{j\ell m})(1+a_*^2)}{A_*^2(1-f)} \right] R = 0, \quad (13)$$

---

<sup>1</sup>The expression we use for  $E_{j\ell m}$  is based on the analysis of [31] but disagrees slightly with the version given there as the sign of the second order term is reversed. This is necessary so that, in the limit  $j, n \rightarrow 0$ , the expression for  $E_{j\ell m}$  correctly reproduces the on-brane eigenvalues that have appeared in the literature previously.

where  $A_*$  and  $K_*$  are given by

$$A_* = (n+1) + (n-1)a_*^2, \quad K_* = (1+a_*^2)\omega_* - a_*m, \quad (14)$$

and

$$D_* \equiv 1 - \frac{4a_*^2}{A_*^2}. \quad (15)$$

By employing the transformation

$$R_{NH}(f) = A_- f^\alpha (1-f)^\beta F(a, b, c; f), \quad (16)$$

equation (13) can be brought to the form of a hypergeometric differential equation [33], with  $a = \alpha + \beta + D_* - 1$ ,  $b = \alpha + \beta$ , and  $c = 1 + 2\alpha$ . In addition, the parameters  $\alpha$  and  $\beta$  are given by

$$\alpha = \pm \frac{iK_*}{A_*}, \quad (17)$$

$$\beta = \frac{1}{2} \left[ (2 - D_*) \pm \sqrt{(D_* - 2)^2 - 4 \left[ \frac{K_*^2 - (j(j+n-1)a_*^2 + \Lambda_{j\ell m})(1+a_*^2)}{A_*^2} \right]} \right]. \quad (18)$$

The general solution of the radial equation (13) may be written in terms of the hypergeometric function  $F$  as follows

$$R_{NH}(f) = A_- f^\alpha (1-f)^\beta F(a, b, c; f) + A_+ f^{-\alpha} (1-f)^\beta F(a-c+1, b-c+1, 2-c; f). \quad (19)$$

In this general near-horizon solution, we must now impose the boundary condition that no outgoing modes exist near the black hole's horizon. In the limit  $r \rightarrow r_h$  we get  $f(r) \rightarrow 0$ , and the near-horizon solution (19) becomes

$$R_{NH}(f) \simeq A_- f^{\pm iK_*/A_*} + A_+ f^{\mp iK_*/A_*} = A_- e^{\pm iky} + A_+ e^{\mp iky}, \quad (20)$$

where

$$k \equiv \omega - m\Omega = \omega - \frac{ma}{r_h^2 + a^2}, \quad (21)$$

and  $y$  is a tortoise-like coordinate defined by  $y = r_h(1+a_*^2) \ln(f)/A_*$ . By imposing this boundary condition, we can set either  $A_- = 0$  or  $A_+ = 0$ , depending on the choice for  $\alpha$ . The two choices are clearly equivalent, so we choose  $\alpha = \alpha_-$ , which imposes  $A_+ = 0$ . This brings the near-horizon solution to the final form

$$R_{NH}(f) = A_- f^\alpha (1-f)^\beta F(a, b, c; f). \quad (22)$$

Finally, the convergence criterion for the hypergeometric function, i.e.  $Re(c-a-b) > 0$ , should also be applied, leading us to choose  $\beta = \beta_-$ .

We now focus our attention on the far-field regime,  $r \gg r_h$ . In this limit, the substitution  $R(r) = r^{-(\frac{n+1}{2})} \tilde{R}(r)$  brings Eq. (8) into the form of a Bessel equation [33], in terms of  $z = \omega r$ ,

$$\frac{d^2 \tilde{R}}{dz^2} + \frac{1}{z} \frac{d\tilde{R}}{dz} + \left( 1 - \frac{E_{j\ell m} + a^2\omega^2 + \left(\frac{n+1}{2}\right)^2}{z^2} \right) \tilde{R} = 0. \quad (23)$$

Thus, the solution in the far-field regime may be written as

$$R_{FF}(r) = \frac{B_1}{r^{\frac{n+1}{2}}} J_\nu(\omega r) + \frac{B_2}{r^{\frac{n+1}{2}}} Y_\nu(\omega r), \quad (24)$$

with  $J_\nu$  and  $Y_\nu$  Bessel functions of the first and second kind, respectively, and  $\nu = \sqrt{E_{j\ell m} + a^2\omega^2 + \left(\frac{n+1}{2}\right)^2}$ .

In order to construct a full analytic solution valid for all  $r$ , we must smoothly match the two asymptotic solutions (22) and (24) in an intermediate regime. To this end, we first focus on the near-horizon solution (22), and shift the argument of the hypergeometric function from  $f$  to  $1 - f$  by using the following relation [33]

$$\begin{aligned} R_{NH}(f) = & A_- f^\alpha (1 - f)^\beta \left[ \frac{\Gamma(c) \Gamma(c - a - b)}{\Gamma(c - a) \Gamma(c - b)} F(a, b, a + b - c + 1; 1 - f) \right. \\ & \left. + (1 - f)^{c-a-b} \frac{\Gamma(c) \Gamma(a + b - c)}{\Gamma(a) \Gamma(b)} F(c - a, c - b, c - a - b + 1; 1 - f) \right]. \end{aligned} \quad (25)$$

The function  $f(r)$  may be alternatively written as

$$f(r) = 1 - \frac{\mu}{r^{n-1}} \frac{1}{r^2 + a^2} = 1 - \left(\frac{r_h}{r}\right)^{n-1} \frac{(1 + a_*^2)}{(r/r_h)^2 + a_*^2}. \quad (26)$$

In the limit  $r \gg r_h$ , the  $(r/r_h)^2$  component in the denominator of the second term dominates, and  $f(r)$  goes to unity for  $n \geq 0$ . Then, the near-horizon solution (26) can be written as

$$R_{NH}(r) \simeq A_1 r^{-(n+1)\beta} + A_2 r^{(n+1)(\beta+D_*-2)}, \quad (27)$$

with  $A_1$  and  $A_2$  defined as

$$\begin{aligned} A_1 &= A_- [(1 + a_*^2) r_h^{n+1}]^\beta \frac{\Gamma(c) \Gamma(c - a - b)}{\Gamma(c - a) \Gamma(c - b)}, \\ A_2 &= A_- [(1 + a_*^2) r_h^{n+1}]^{-(\beta+D_*-2)} \frac{\Gamma(c) \Gamma(a + b - c)}{\Gamma(a) \Gamma(b)}. \end{aligned} \quad (28)$$

Next, we expand the far-field solution to small values of  $r$ , by taking the limit  $r \rightarrow 0$  in Eq. (24) :

$$R_{FF}(r) \simeq \frac{B_1 \left(\frac{\omega r}{2}\right)^\nu}{r^{\frac{n+1}{2}} \Gamma(\nu + 1)} - \frac{B_2}{\pi r^{\frac{n+1}{2}}} \frac{\Gamma(\nu)}{\left(\frac{\omega r}{2}\right)^\nu}. \quad (29)$$

Then, taking the small  $a_*$  and  $\omega_*$  limit in the power coefficients of  $r$  – so that we can ignore terms of order  $(\omega_*^2, a_*^2, a_*\omega_*)$  or higher – we can achieve exact matching since

$$\begin{aligned} -(n+1)\beta &\simeq \ell + \mathcal{O}(\omega_*^2, a_*^2, a_*\omega_*), \\ (n+1)(\beta + D_* - 2) &\simeq -(\ell + n + 1) + \mathcal{O}(\omega_*^2, a_*^2, a_*\omega_*), \\ \nu &\simeq \ell + \frac{n+1}{2} + \mathcal{O}(a_*^2\omega_*^2). \end{aligned} \quad (30)$$

We would like to stress here that, in order to achieve a higher level of accuracy in our analysis, no expansion is performed in the arguments of the gamma functions, and terms to order  $(a\omega)^4$  are retained in the expansion of the eigenvalues. Then, the matching of the two asymptotic solutions leads to the constraint

$$B \equiv \frac{B_1}{B_2} = -\frac{1}{\pi} \left( \frac{2}{\omega r_h (1 + a_*^2)^{\frac{1}{n+1}}} \right)^{2\ell+n+1} \sqrt{E_{j\ell m} + a^2 \omega^2 + \left( \frac{n+1}{2} \right)^2} \\ \times \frac{\Gamma^2 \left( \sqrt{E_{j\ell m} + a^2 \omega^2 + \left( \frac{n+1}{2} \right)^2} \right) \Gamma(\alpha + \beta + D_* - 1) \Gamma(\alpha + \beta) \Gamma(2 - 2\beta - D_*)}{\Gamma(2\beta + D_* - 2) \Gamma(2 + \alpha - \beta - D_*) \Gamma(1 + \alpha - \beta)}. \quad (31)$$

The above guarantees the existence of a smooth, analytic solution for the radial part of the wavefunction for all  $r$ , valid in the low-energy and low-rotation limit.

## 4 The Absorption Probability

With the solution to the radial equation (8) at our disposal, we may now compute the absorption probability. To this end, we expand the far-field solution (23) for  $r \rightarrow \infty$ . By using standard formulae for the Bessel functions [33], we find

$$R_{FF}(r) \simeq \frac{1}{r^{\frac{n+2}{2}} \sqrt{2\pi\omega}} \left[ (B_1 + iB_2) e^{-i(\omega r - \frac{\pi}{2}\nu - \frac{\pi}{4})} + (B_1 - iB_2) e^{i(\omega r - \frac{\pi}{2}\nu - \frac{\pi}{4})} \right] \\ = A_{in}^{(\infty)} \frac{e^{-i\omega r}}{r^{\frac{n+2}{2}}} + A_{out}^{(\infty)} \frac{e^{i\omega r}}{r^{\frac{n+2}{2}}}. \quad (32)$$

We see that for large distances from the black hole, the solution reduces to an incoming and an outgoing spherical wave, allowing us to compute the absorption probability from the ratio of their amplitudes:

$$|\mathcal{A}_{j\ell m}|^2 = 1 - \left| \frac{A_{out}^{(\infty)}}{A_{in}^{(\infty)}} \right|^2 = 1 - \left| \frac{B_1 - iB_2}{B_1 + iB_2} \right|^2 = \frac{2i(B^* - B)}{BB^* + i(B^* - B) + 1}. \quad (33)$$

The above equation, in conjunction with Eq. (31), is our main analytic result for the absorption probability characterising the emission of massless scalar fields in the bulk, from a rotating, uncharged black hole, in the low-energy and low-angular momentum limit.

In Fig. (1) we plot the absorption probability for the first partial waves for  $n = 2$ ,  $a_* = 0.4$ , with the values of  $j, \ell, m$  obeying the restrictions (11). One may easily observe the dominance of the first partial wave  $j = \ell = m = 0$  over all others, and the suppression of  $|\mathcal{A}_{j\ell m}|^2$  as the values of the angular momentum numbers increase. In the plot, we also see the appearance of superradiance [34] for modes with positive  $m$ , where the absorption probability takes negative values. Figure (1) actually depicts two sets of curves: the first, denoted by solid lines, gives the value of  $|\mathcal{A}_{j\ell m}|^2$  that follows from our analytic result (33), while the second set, denoted by dashed lines, gives the value following from integrating

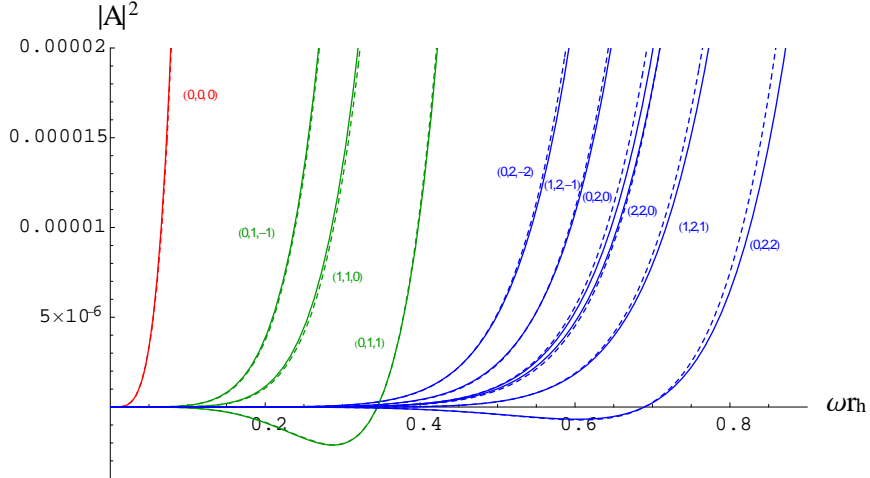


Figure 1: Absorption probabilities  $|\mathcal{A}_{j\ell m}|^2$  for a bulk scalar field, for  $n = 2$ ,  $a_* = 0.4$ , and various combinations of  $(j, \ell, m)$ .

the radial equation (8) numerically<sup>2</sup>. As in the case of scalar [27] and higher-spin fields [28] propagating on the brane, our approximate analytic method leads to results that are in excellent agreement with the exact numerical ones, not only in the low-energy regime but beyond this also.

Focusing on the dominant first partial wave, in Fig. 2(a) we demonstrate the dependence of the absorption probability on the rotation parameter  $a_*$ , for fixed  $n = 5$ . One may clearly see that an increase in the rotation of the black hole causes an enhancement in the value of  $|\mathcal{A}_{j\ell m}|^2$  in the low- and intermediate-energy regimes. In Fig. 2(b), we investigate instead the effect of the number of extra dimensions on the value of the absorption probability, while we fix  $a_* = 0.5$ . As is clear from the plot, the value of  $|\mathcal{A}_{j\ell m}|^2$  in the low-energy regime is strongly suppressed as  $n$  increases. The same behaviour in terms of  $n$  was found for bulk scalar fields propagating in the background of a higher-dimensional, spherically-symmetric black hole [8].

An interesting question is how the absorption probabilities for brane and bulk scalar fields in a rotating black-hole background compare. By examining the results presented in this section and in [27], one may easily conclude that the absorption probabilities for both species of scalar fields are enhanced as the black hole rotation parameter increases. In contrast to this, the value of the absorption probability increases with  $n$  for brane scalars, while it decreases for bulk scalar fields. Important conclusions can also be drawn by directly comparing Fig. 1 with the corresponding figure in [27]: for the same values of  $n$  and  $a_*$ , the absorption probability for brane scalar fields is consistently larger than that for bulk scalars by almost 3 orders of magnitude, both for superradiant and non-superradiant modes. The same observation was made in [23] in the 5-dimensional case – here, we have shown that this behaviour persists for higher values of  $n$  also.

<sup>2</sup>In the numerical integration of Eq. (8) the power series expansion of the eigenvalue  $E_{j\ell m}$  [31] up to 5th order, valid in the low- $a\omega$  limit, was again used.



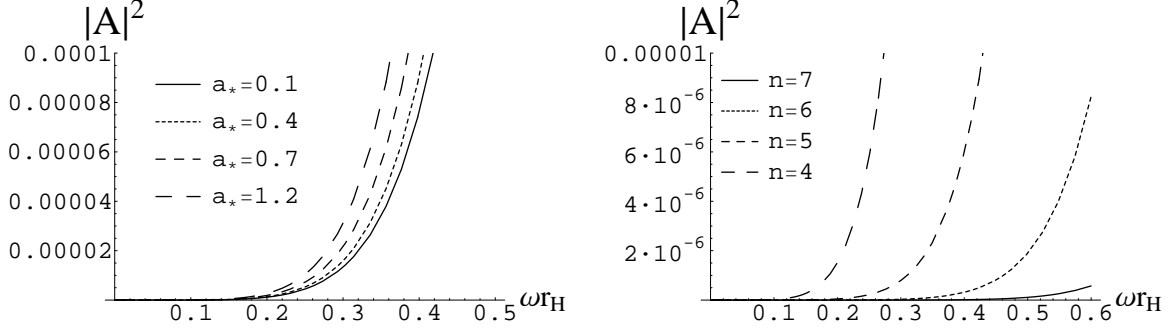


Figure 2: Absorption probabilities for the bulk scalar mode  $j = \ell = m = 0$ , for (a)  $n = 5$  and various  $a_*$ , and (b)  $a_* = 0.5$  and various  $n$ .

A compact analytic expression for the absorption probability may be derived in the very low-energy limit. For  $\omega \rightarrow 0$ , we obtain  $B \propto 1/\omega^{2\ell+n+1}$ , therefore

$$|\mathcal{A}_{j\ell m}|^2 \simeq 2i \left( \frac{1}{B} - \frac{1}{B^*} \right). \quad (34)$$

Substituting for  $B$  from Eq. (31), we take

$$|\mathcal{A}_{j\ell m}|^2 = \frac{-2i\pi (\omega r_h/2)^{2\ell+n+1}}{(\ell + \frac{n+1}{2}) \Gamma^2(\ell + \frac{n+1}{2}) (1 + a_*^2)^{-\frac{2\ell+n+1}{n+1}} \Gamma(2 - 2\beta - D_*)} \times \left[ \frac{\Gamma(2 + \alpha - \beta - D_*) \Gamma(1 + \alpha - \beta)}{\Gamma(\alpha + \beta + D_* - 1) \Gamma(\alpha + \beta)} - \frac{\Gamma(2 - \alpha - \beta - D_*) \Gamma(1 - \alpha - \beta)}{\Gamma(-\alpha + \beta + D_* - 1) \Gamma(-\alpha + \beta)} \right].$$

Focusing our attention on the dominant mode  $j = \ell = m = 0$ , and performing an analysis similar to that in [27], where the absorption probability of the dominant scalar mode on the brane was found in the same limit, we obtain the result

$$|\mathcal{A}_0|^2 = \frac{4\pi(1 + a_*^2)^2(\omega r_h)^{n+2}}{A_* 2^n(n+1)\Gamma^2\left(\frac{n+1}{2}\right)(2 - D_*)} + \dots \quad (35)$$

The above result allows us also to compute the absorption cross-section  $\sigma_0$  for the dominant scalar bulk mode in the asymptotic low-energy regime. By adapting the formula of Ref. [35] to the geometrical set-up of our analysis, we may write

$$\sigma_{j\ell m}(\omega) = \frac{2^n}{\pi} \Gamma^2\left(\frac{n+3}{2}\right) \frac{A_H}{(\omega r_h)^{n+2}} \frac{N_j}{(1 + a_*^2)} |\mathcal{A}_{j\ell m}|^2, \quad (36)$$

where now

$$N_j = \frac{(2j + n - 1)(j + n - 2)!}{j!(n-1)!}, \quad A_H = \frac{2\pi^{\frac{n+3}{2}} r_h^n (r_h^2 + a^2)}{\Gamma\left(\frac{n+3}{2}\right)} \quad (37)$$

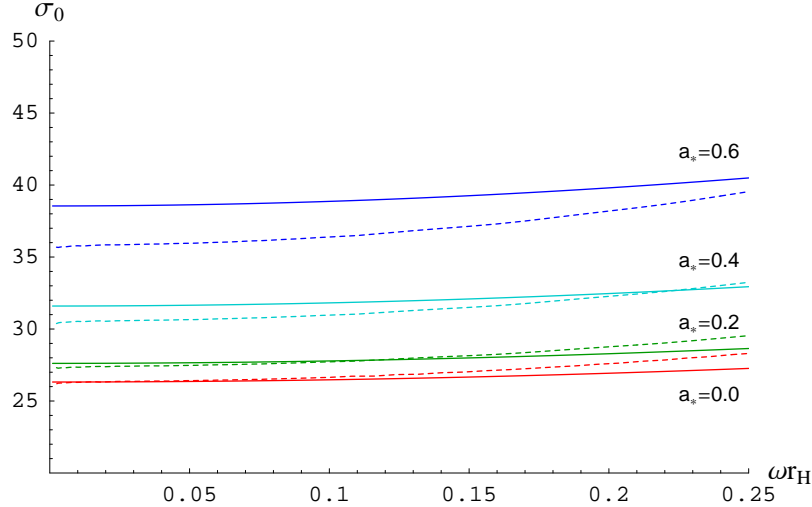


Figure 3: Absorption cross-section for the bulk scalar mode  $j = \ell = m = 0$ , for  $n = 2$  and various values of  $a_*$ .

are the multiplicity of the  $j$ th partial wave in the expansion of the wave function over the hyperspherical harmonics on the  $n$ -sphere, and the horizon area of the  $(4+n)$ -dimensional rotating black hole, respectively. Substituting for the absorption coefficient, we obtain

$$\sigma_0(\omega) \simeq \frac{(n+1)(1+a_*^2)A_H}{A_*(2-D_*)} + \dots \quad (38)$$

For  $a_* \rightarrow 0$ , the above reduces to  $A_H$ , a behaviour that was found in [8]. For  $a_* \neq 0$ , the numerical results (dashed lines) presented in Fig. 3 confirm that, also here, the low-energy limit of the cross-section tends to the area of the corresponding rotating black hole. The solid lines demonstrate the agreement of our analytic results with the numerical ones for small values of  $a_*$ , and the expected deviation for large values of the rotation parameter.

## 5 Energy Emission Rate

Having found the absorption probability (Eq. 33), we can now proceed to compute the rate of energy emission of massless scalar fields in the bulk. This is given by the expression

$$\frac{d^2 E}{dt d\omega} = \frac{1}{2\pi} \sum_{j,\ell,m} \frac{\omega}{\exp[k/T_H] - 1} N_j |\mathcal{A}_{j\ell m}|^2. \quad (39)$$

The above differs from the 4-dimensional [36] expression in the presence of an additional sum over the new angular momentum number  $j$ , and from the 5-dimensional [17] one in the introduction of the multiplicity of states  $N_j$  (37) following from the expansion of the wavefunction of the field in the  $n$ -dimensional sphere. The parameter  $k$  is defined in Eq. (21), while the temperature of the higher-dimensional, rotating black hole is

$$T_H = \frac{(n+1) + (n-1)a_*^2}{4\pi(1+a_*^2)r_h}. \quad (40)$$

A useful check that may convince us of the validity of the above emission rate is to take the non-rotating limit. Then, Eq. (39) for the energy rate should reduce to the well-known result for bulk scalar emission from a  $(4+n)$ -dimensional Schwarzschild black hole [7, 8]

$$\frac{d^2 E}{dt d\omega} = \frac{1}{2\pi} \sum_{\ell} \frac{\omega}{\exp[\omega/T_H] - 1} N_{\ell} |\mathcal{A}_{\ell}|^2, \quad (41)$$

where now  $N_{\ell}$  is the degeneracy of the  $\ell$ th mode of the harmonics on the  $(n+2)$ -sphere

$$N_{\ell} = \frac{(2\ell + n + 1)(\ell + n)!}{\ell!(n+1)!}. \quad (42)$$

In the limit  $a \rightarrow 0$ , we get  $k = \omega$ , and the absorption probability becomes independent of both  $m$  and  $j$ , retaining a dependence only on the principal quantum number  $\ell$ . Then, Eq. (39) matches Eq. (41) providing the following relation holds

$$\sum_{j,m} N_j = \sum_{j=0}^{\ell} (\ell - j + 1) \frac{(2j + n - 1)(j + n - 2)!}{j!(n-1)!} \equiv N_{\ell}. \quad (43)$$

In the second part of the above equation, we have used the fact that, according to the restrictions (11) imposed on the quantum numbers, for each value of  $(j, \ell)$ ,  $m$  may take  $\ell - j + 1$  values, and for each value of  $\ell$ ,  $j$  may take the values  $0 \leq j \leq \ell$ . In order to prove Eq. (43), we rewrite the factor  $2j + n - 1$  as  $(j + n - 1) + j$ , and split the sum in two parts. Then, if we further replace the index  $j$  by  $i - n + 1$  in the first sum and by  $i - n + 2$  in the second, the middle part of Eq. (43) takes the form

$$\sum_{i=n-1}^{\ell+n-1} (\ell + n - 1 - i + 1) C(i, n - 1) + \sum_{i=n-1}^{\ell+n-2} (\ell + n - 2 - i + 1) C(i, n - 1), \quad (44)$$

where  $C(s, r)$  is the combination function,  $C(s, r) = \frac{s!}{r!(s-r)!}$ . By using the identity

$$\sum_{i=r}^s (s - i + 1) C(i, r) = C(s + 2, r + 2), \quad (45)$$

the first sum in Eq. (44) reduces to  $C(\ell + n + 1, n + 1)$ , and the second to  $C(\ell + n, n + 1)$  - their sum can be easily shown to equal  $N_{\ell}$ .

By using Eq. (39), in Figs. 4(a,b), we plot the energy emission rate for a higher-dimensional rotating black hole in the form of bulk scalar fields, as a function of the energy parameter  $\omega r_h$ , and in terms of the angular momentum parameter and number of extra dimensions, respectively. The profile exhibited by the absorption probability is also observed here: the emission rate is enhanced with  $a_*$  in the low-energy regime, in analogy with results for brane scalars, fermions and gauge bosons [20, 21, 24, 25, 26, 27, 28], while is suppressed in terms of  $n$ . Drawing experience from previous studies, we expect the enhancement in terms of  $a_*$  to persist over the whole energy regime - on the other hand, it is quite likely, given the similarity of the results with those for bulk scalar fields

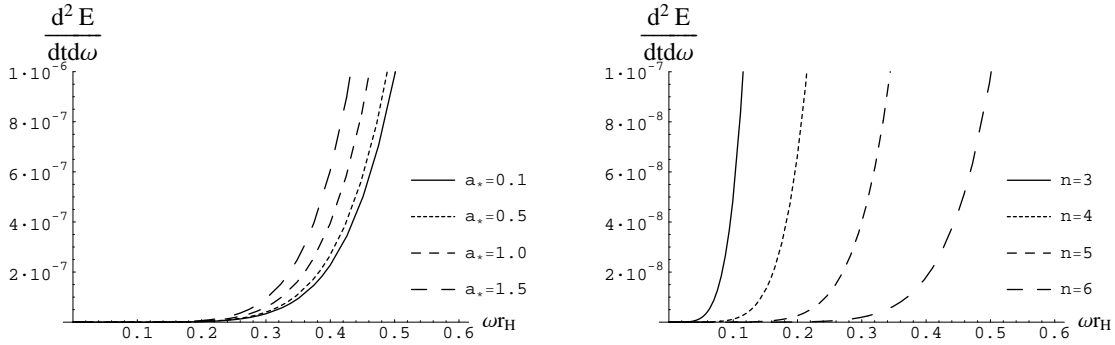


Figure 4: Energy emission rates for bulk scalar fields **(a)** for  $n = 5$  and various  $a_*$ , and **(b)** for  $a = 0.5$  and various  $n$ .

in a non-rotating background [8], that the low-energy suppression with  $n$  will be replaced by a strong enhancement at the high-energy regime.

We should finally address the question of the brane-to-bulk ratio of the rate of scalar field energy emission from a higher-dimensional rotating black hole. The answer to this question is important as it will define the amount of energy spent by the black hole in the observable brane channel. Whereas the energy emission rate for bulk scalars is given by Eq. (39), the corresponding one for brane scalar degrees of freedom is [18, 20, 26, 21]

$$\frac{d^2 E}{dt d \omega} = \frac{1}{2\pi} \sum_{\ell, m} \frac{\omega}{\exp[k/T_H] - 1} |\mathcal{A}_{\ell m}|^2. \quad (46)$$

The comparison between the bulk and brane absorption probabilities discussed in the previous section has given a clear signal as to which emission is dominant, however the final comparison should involve the total emission rates where the different multiplicities of states have been taken into account. By using Eqs. (39) and (46), the brane-to-bulk ratio for scalar fields from a rotating black hole is depicted in Figs. 5(a,b) in terms of the parameters  $a_*$  and  $n$ . We may easily observe that although the exact value is both  $a_*$  and  $n$ -dependent, the ratio of the brane to bulk emission rates always remains above unity, rendering the brane channel dominant. We remind the reader that a similar conclusion was also drawn in the case of a Schwarzschild-like higher-dimensional black hole [8].

## 6 Conclusions

In this work we have performed an analytic study of the emission of scalar fields in the bulk from a higher-dimensional rotating black hole. By solving analytically the radial part of the equation of the scalar field, we have constructed a smooth solution, valid in the low-energy and low-angular-momentum regime. We were then able to compute the corresponding absorption probability, and to examine its behaviour in terms of the particle's angular momentum numbers and spacetime properties. The lowest scalar mode was found to be dominant, with its absorption cross-section equal to the horizon of the

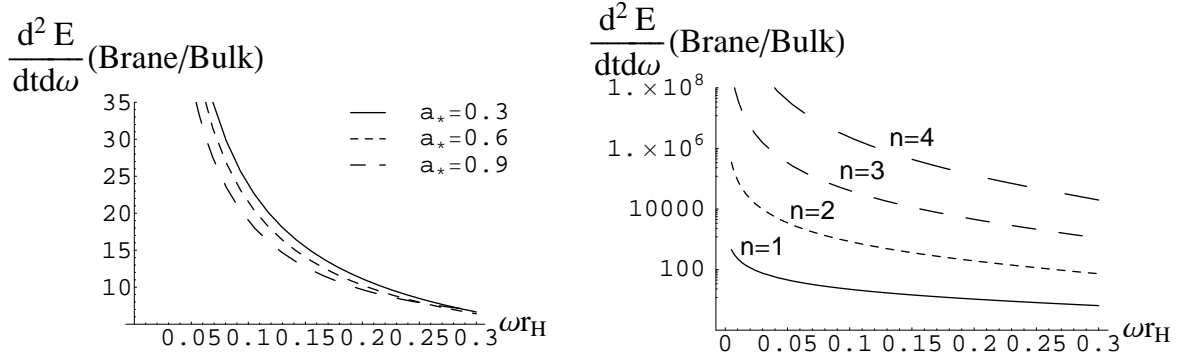


Figure 5: Brane-to-bulk ratio of the energy emission rates for scalar fields (a) for  $n = 1$  and various  $a_*$ , and (b) for  $a = 0.5$  and various  $n$

higher-dimensional rotating black hole in the extreme low-energy limit. We demonstrated that the absorption probability for bulk scalar fields is enhanced with increasing angular momentum of the black hole and suppressed by the number of extra dimensions. We also performed a numerical analysis, valid again in the low- $\omega$  and low- $a_*$  regime, and showed that our analytic results are in excellent agreement with the exact numerical ones even up to intermediate-energy regimes.

We then computed the energy emission rate in the bulk, and showed that it exhibits the same behaviour as the absorption probability in terms of  $a_*$  and  $n$ . Finally, we calculated the brane-to-bulk ratio of energy emission rates for scalar fields in a rotating, higher-dimensional background and found that, in the low- $\omega$  and low- $a_*$  regime, it is always larger than unity. This is due to the fact that the larger multiplicity of scalar states in the bulk cannot counteract the fact that the bulk absorption probability is approximately three orders of magnitude smaller than the corresponding brane value in the low energy limit. It is this dominance of the brane absorption probability that largely determines the preference of the black hole to emit scalar field energy on the brane. The complete radiation spectrum – that may follow only from an exact, numerical analysis involving both the angular and radial parts of the field equation – is necessary to decide whether the brane-to-bulk ratio remains above unity over the entire frequency range.

**Acknowledgments.** P.K. is grateful to M. Casals, S. Dolan and E. Winstanley for useful discussions. S.C and O.E. acknowledge PPARC and I.K.Y. fellowships, respectively. P.K. is funded by the UK PPARC Research Grant PPA/A/S/2002/00350. K.T. and P.K. acknowledge participation in the RTN networks UNIVERSENET-MRTN-CT-2006035863-1 and MRTN-CT-2004-503369.

## References

- [1] N. Arkani-Hamed, S. Dimopoulos and G. R. Dvali, *Phys. Lett. B* **429**, 263 (1998); *Phys. Rev. D* **59**, 086004 (1999); I. Antoniadis, N. Arkani-Hamed, S. Dimopoulos

- and G. R. Dvali, *Phys. Lett. B* **436**, 257 (1998).
- [2] L. Randall and R. Sundrum, *Phys. Rev. Lett.* **83** (1999) 3370; *Phys. Rev. Lett.* **83** (1999) 4690.
- [3] T. Banks and W. Fischler, hep-th/9906038;  
R. Emparan, G. T. Horowitz and R. C. Myers, *Phys. Rev. Lett.* **85** (2000) 499;  
D. M. Eardley and S. B. Giddings, *Phys. Rev. D* **66**, 044011 (2002);  
H. Yoshino and Y. Nambu, *Phys. Rev. D* **66**, 065004 (2002); *ibid.* **D 67**, 024009 (2003);  
E. Kohlprath and G. Veneziano, *JHEP* **0206**, 057 (2002);  
V. Cardoso, O. J. C. Dias and J. P. S. Lemos, *Phys. Rev. D* **67**, 064026 (2003);  
E. Berti, M. Cavaglia and L. Gualtieri, *Phys. Rev. D* **69**, 124011 (2004);  
S. B. Giddings and V. S. Rychkov, *Phys. Rev. D* **70**, 104026 (2004);  
H. Yoshino and V. S. Rychkov, *Phys. Rev. D* **71** (2005) 104028 ;  
D. C. Dai, G. D. Starkman and D. Stojkovic, *Phys. Rev. D* **73** (2006) 104037 ;  
H. Yoshino and R. B. Mann, *Phys. Rev. D* **74** (2006) 044003 ;  
H. Yoshino, T. Shiromizu and M. Shibata, *Phys. Rev. D* **74**, 124022 (2006).
- [4] F. R. Tangherlini, *Nuovo Cim.* **27**, 636 (1963);  
R. C. Myers and M. J. Perry, *Annals Phys.* **172**, 304 (1986).
- [5] S. W. Hawking, *Commun. Math. Phys.* **43**, 199 (1975).
- [6] P. Kanti, *Int. J. Mod. Phys. A* **19** (2004) 4899; E. Winstanley, arXiv:0708.2656 [hep-th].
- [7] P. Kanti and J. March-Russell, *Phys. Rev. D* **66**, 024023 (2002); *Phys. Rev. D* **67**, 104019 (2003).
- [8] C. M. Harris and P. Kanti, *JHEP* **0310** (2003) 014.
- [9] A. Barrau, J. Grain and S. O. Alexeyev, *Phys. Lett. B* **584**, 114 (2004); J. Grain, A. Barrau and P. Kanti, *Phys. Rev. D* **72**, 104016 (2005); T. G. Rizzo, *Class. Quant. Grav.* **23**, 4263 (2006).
- [10] E. I. Jung, S. H. Kim and D. K. Park, *Phys. Lett. B* **586** (2004) 390; *JHEP* **0409** (2004) 005; *Phys. Lett. B* **602** (2004) 105; *Phys. Lett. B* **614** (2005) 78; E. Jung and D. K. Park, *Nucl. Phys. B* **717** (2005) 272; hep-th/0506204.
- [11] P. Kanti, J. Grain and A. Barrau, *Phys. Rev. D* **71** (2005) 104002.
- [12] A. S. Cornell, W. Naylor and M. Sasaki, *JHEP* **0602** (2006) 012.
- [13] D. K. Park, *Class. Quant. Grav.* **23** (2006) 4101.
- [14] V. Cardoso, M. Cavaglia and L. Gualtieri, *Phys. Rev. Lett.* **96**, 071301 (2006) [Erratum-*ibid.* **96**, 219902 (2006)]; *JHEP* **0602**, 021 (2006).
- [15] S. Creek, O. Efthimiou, P. Kanti and K. Tamvakis, *Phys. Lett. B* **635** (2006) 39; O. Efthimiou, hep-th/0609144.

- [16] D. C. Dai, N. Kaloper, G. D. Starkman and D. Stojkovic, *Phys. Rev. D* **75**, 024043 (2007).
- [17] V. P. Frolov and D. Stojkovic, *Phys. Rev. D* **67**, 084004 (2003).
- [18] D. Ida, K. y. Oda and S. C. Park, *Phys. Rev. D* **67**, 064025 (2003) [Erratum-ibid. *D* **69**, 049901 (2004)].
- [19] H. Nomura, S. Yoshida, M. Tanabe and K. i. Maeda, *Prog. Theor. Phys.* **114**, 707 (2005).
- [20] C. M. Harris and P. Kanti, *Phys. Lett. B* **633**, 106 (2006).
- [21] D. Ida, K. y. Oda and S. C. Park, *Phys. Rev. D* **71**, 124039 (2005); *Phys. Rev. D* **73**, 124022 (2006).
- [22] E. Jung, S. Kim and D. K. Park, *Phys. Lett. B* **615**, 273 (2005); *Phys. Lett. B* **619**, 347 (2005);
- [23] E. Jung and D. K. Park, *Nucl. Phys. B* **731**, 171 (2005).
- [24] G. Duffy, C. Harris, P. Kanti and E. Winstanley, *JHEP* **0509**, 049 (2005).
- [25] M. Casals, P. Kanti and E. Winstanley, *JHEP* **0602**, 051 (2006).
- [26] M. Casals, S. R. Dolan, P. Kanti and E. Winstanley, *JHEP* **0703**, 019 (2007).
- [27] S. Creek, O. Efthimiou, P. Kanti and K. Tamvakis, *Phys. Rev. D* **75** (2007) 084043.
- [28] S. Creek, O. Efthimiou, P. Kanti and K. Tamvakis, arXiv:0707.1768 [hep-th], to appear in *Phys. Rev. D*.
- [29] C. Muller, in *Lecture Notes in Mathematics: Spherical Harmonics* (Springer-Verlag, Berlin-Heidelberg, 1966).
- [30] D. Ida, Y. Uchida and Y. Morisawa, *Phys. Rev. D* **67** (2003) 084019 .
- [31] E. Berti, V. Cardoso and M. Casals, *Phys. Rev. D* **73** (2006) 024013 [Erratum-ibid. *D* **73** (2006) 109902];
- [32] V. Cardoso, G. Siopsis and S. Yoshida, *Phys. Rev. D* **71**, 024019 (2005).
- [33] M. Abramowitz and I. Stegun, *Handbook of Mathematical Functions* (Academic, New York, 1996).
- [34] Y.B. Zel'dovich, *JETP Lett.* **14**, 180 (1971).
- [35] S. S. Gubser, I. R. Klebanov and A. A. Tseytlin, *Nucl. Phys.* **B499**, 217 (1997); S. D. Mathur, *Nucl. Phys. B* **514**, 204 (1998); S. S. Gubser, *Phys. Rev. D* **56**, 4984 (1997).
- [36] A. C. Ottewill and E. Winstanley, *Phys. Rev. D* **62**, 084018 (2000).